A Comparitive Study of the MSI and Proba-V linear Arrays under the Influence of Radiation.

AMICSA 2012

26-28 August 2012

Jonas Bentell[(1)], Koen van der Zanden[(1)], Thierry Colin[(1)], Siegfried Herftijd[(1)], Patrick Merken[(1),(2)], Jan Vermeiren [(1)]

[(1)]Xenics nv
Ambachtenlaan 44 – BE-3001 Leuven Belgium
Email: Jan.vermeiren@xenics.com
[(2)]RMA
Renaissancelaan 30 – BE-1000 Brussel, Belgium
Email: patrick.merken@rma.ac.be

INTRODUCTION

For vegetation and ocean colour monitoring studies, wavelength bands in the visible, NIR and SWIR realm are very important instruments. For both the Proba-V instrument [1], as the Multispectral Instrument (MSI) on Earthcare [2] [3], several pushbroom imagers are developed for signal acquisition in the 680 and 860 nm, 1.55 and 2.2 µm bands.
The diversity of ROICs, CMOS technologies and sensor materials offers a good opportunity to compare the effects of radiation, being ionizing ^{60}Co, low and high energy protons and heavy ions during qualification testing and to draw conclusions about the origin and the mechanisms of radiation effects.

Selection and Discussion of detector materials fot MSI.

Table 1 provides the details for the PDA's in the MSI instrument. In order to avoid interference effects in the toplayers of the PDA and hence variations in the external quantum efficiency, all PDA types are designed with a well-controlled single layer Anti-reflective coating [4-7].

Table 1: Material selection and detector design parameters for the VNS detectors. (ρ_{ToA}: Reflectivity at **T**op **o**f **A**tmosphere)

Channel	Wavelength	Material	$T_{detector}$	SNR@100%ρ_{ToA}
VIS	$0.67^{\pm 0.01}$ µm	Si, p-on-n, 11.5 µm epi, optimized AR	Room temp	500
NIR	$0.865^{\pm 0.01}$ µm	Si, p-on-n, 11.5 µm epi, optimized AR	Room temp	500
SWIR1	$1.55^{\pm 0.015}$ µm	$In_{0.47}Ga_{0.53}As$ grown on InP	Room temp	250
SWIR2	$2.21^{\pm 0.015}$ µm	Extended InGaAs on buffer layer	[230-240 K]	250

FPA and ROIC Architecture for the MSI mission

All detectors are mounted in a metal can package. The Photodiode array (PDA) is placed in the middle of the package on a substrate. The PDA contains 512 pixels on a pitch of 25 µm, which are wire bonded to 2 CMOS ROIC's with 256 inputs each on a pitch of 50 µm. The 2 ROICs are also placed on the alumina substrate together with 4 screen printed resistors in a rad hard process [8] [9].

The ROIC is realized in the C05A technology of ON Semi in Oudenaarde, Belgium. This process is characterized by 2 poly layers and 3 metal layers. The nominal supply voltage is 5 V.

The analogue signal path consists of a Charge sensitive TransImpedance Amplifier or CTIA with 4 different charge to voltage conversion settings. The OTA (Operational Transconductance Amplifier) is designed as a truly differential amplifier. All photodiodes (Silicon as well as InGaAs) have p- junctions in a n-type substrate. At the end of the integration cycle the information is transferred to a Sample and Hold stage before the sequential readout starts. The device can be operated in an Integrate-Than-Read (ITR) or Integrated-While-Read mode (IWR) [9] [10].

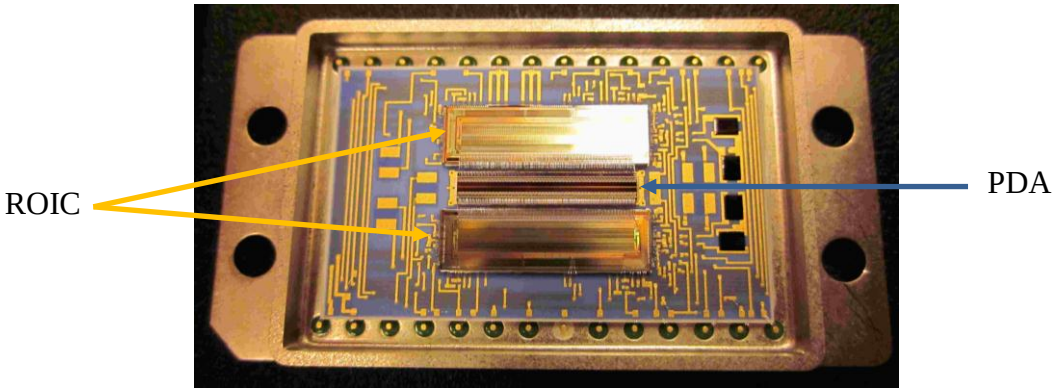

Figure 1: Photograph of uncapped linear array assembly with central PDA, 2 ROICs and auxiliary passive components.

The device was originally designed for low-ohmic extended InGaAs detectors with a specific shunt resistance as low as 150 – 300 Ω.cm2 at the detector operating temperature < 250 K. For this purpose an auto-zero circuit was introduced in the CTIA stage, which reduced the V_T non-uniformity and hence the detector bias uniformity to a level of app. 10 µV. Another benefit of the increased bias uniformity is that the PDA can be operated effectively at zero bias, eliminating the dark current and the dark current non-uniformity.

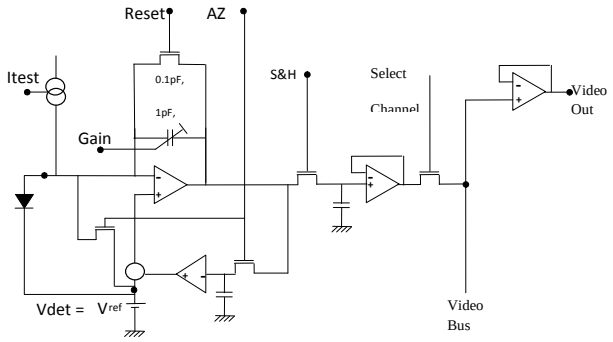

Figure 2: Schematic capture of the analogue signal chain for the MSI ROIC.

In each CTIA a test current can be injected in order to test the ROIC before assembly. The CTIA has 4 selectable feed-back capacitors, resulting in sensitivity of resp. 1600, 160, 20 and 10 nV/e^-. For the characterisation and the mission, mainly the 0.1 and 1 pF capacitors will be used. The noise varies between 0.45 and 7 mV_{rms} for the 16 and 0.1 pF capacitor, respectively.

FPA and ROIC Architecture for the Proba-V mission.

The SWIR detector for the Proba-V mission is also mounted in a metal can package. Due to the pixel count and the length of the PDA it was decided to go for a mechanically overlapping configuration. In
Figure 3, the overall geometry of the FPA is shown; in order to avoid gaps, the 3 arrays are placed in an overlapping arrangement.

Due to the limited along-track FOV of the Proba-V telescope [11], the distance of the PD rows had to be limited to < 1.5 mm. A single layer of bonding wires with a pitch of 50 µm is proven to give good interconnection yield. By using a double wire bonding bridge, the PD's could be designed on a pitch of 25 µm.
The number of PDA subarrays is a compromise between the pixel yield and the difficulties in assembling the subarrays in the overall FPA. Finally, an approach with 3 subarrays of 1024 pixels is selected with [70-100 pixels] in the overlap area. This configuration results in an overall array length of >2752 pixels.

The ROICs are realized in the C035A technology of ON Semi in Oudenaarde, Belgium. This process is characterized by 2 poly layers and 5 metal layers. The nominal supply voltage is 3.3 V.

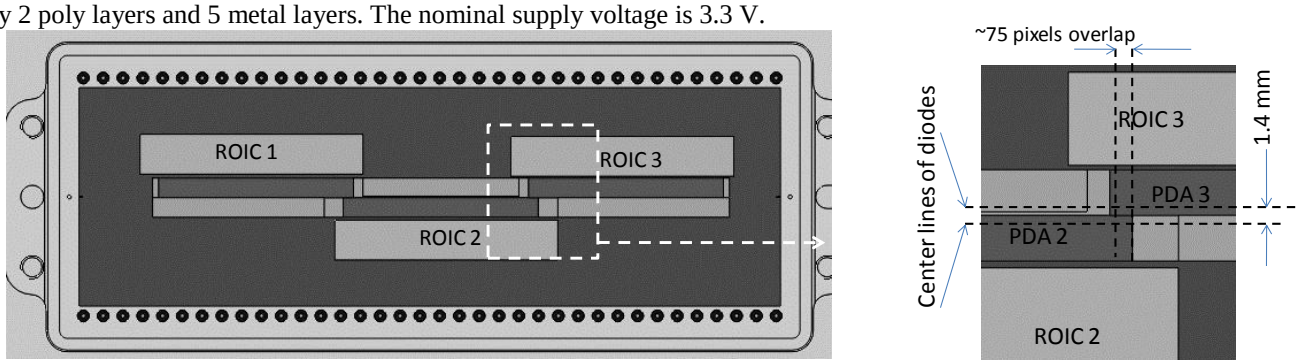

Figure 3: Outline of device in package without lid and window. Left: The three ROICs and PDAs placed inside the package. Right: Partial overlap between the PDAs. The horizontal dotted lines show the off-centre location of the line of photosensitive elements, the off-centre location of the line of photosensitive elements, their distances and the overlap between two PDA chips.

The detector interface circuit is again a CTIA. Contrary to the previous discussed circuit, this CTIA stage has no AutoZero stage, but the careful design allows operating the photodiodes with a constant backbias ≤ 100 mV [6], [12], [13]

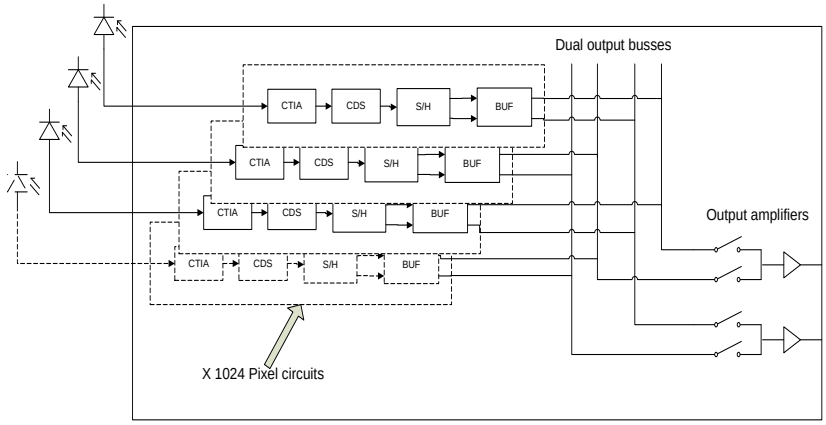

Figure 4: Overview of the analogue signal chain of the Proba-V ROIC.

The overall analogue chain is depicted in Figure 4 and contains besides the CTIA stage the following elements:

- Correlated Double Sampling (CDS), applied in a separate gain stage: to reduce the influence of kTC-noise [14].
- For IWR mode, the next step is the Sample-and-Hold stage (S/H), including a single ended to differential conversion.
- The column buffers, which multiplexes the signals onto two output busses.

Each ROIC contains 1024 pixel interface stages in parallel.
Finally, a low impedance output amplifier is used to drive the external load.

The CTIA is designed with 5 individually selectable capacitors of 5, 25, 100, 200 and 500 fF. The sensitivities are ranging between 0.19 and 32 µV/e-. The noise varies between 20 and 0.8 mV_{rms} for the 5 and 830fF capacitor, respectively.

RADIATION TESTING

Radiation conditions.

All arrays were irradiated without lid; i.e. in worst case conditions. They were subject to 3 different types of radiation:

- ^{60}Co ionizing radiation

- Protons, with low and high energy,
- Heavy ions, mainly Ne, Ar, Kr and Xe

Most of the FPAs were irradiated in the ESTEC ^{60}Co facility in Noordwijk, Nl with a dose rate of 1500 Rad(Si)/h for a total accumulated dose of 10 krad(Si). Some SWIR1 devices of the MSI type were also tested in the SCK, Mol-Belgium facility: the radiation started at 180 rad(Si)/h and gradual increased to 360 rad(Si)/h; the total radiation time was 11 h, equivalent to 10 krad(Si)

During proton irradiation 2 different experiments were executed. Firstly high proton energies (150 and 190 MeV) were used in order to provoke SEE and more specifically latch-up in the ROIC.
Then another part of the FPA was subject to low energy protons with E = 30 MeV for dark current degradation. At this energy a fluence of 10^{10} p^+/cm^2 corresponds a total dose of ≈ 2.3 krad(Si). [15]

Heavy ions were mainly used to study the SEE. For this purpose Ne, Ar, Kr and Xe ions were used at different energies and incidence angles to create LET (Linear Energy Transfer) values in the range [6.20 – 67.70 MeV.cm^2/mg(Si)]. Radiation was continued till app. 175 SEE's were detected or till a total fluence of 10^7 ions/cm2 was reached. A summary of the different test campaigns is given in Table 2.

Table 2: Summary of the different radiation campaigns on the MSI and Proba-V FPA's

Array type	^{60}Co	p^+	Heavy Ion
Proba-V SWIR1	ESTEC, Noordwijk, NL	KVI, Groningen, NL	HIF, UCL, B
MSI RED	ESTEC, Noordwijk, NL	KVI, Groningen, NL	
MSI NIR	ESTEC, Noordwijk, NL	KVI, Groningen, NL	
MSI SWIR1	SCK, Mol-B ESTEC, Noordwijk, NL	PROSCAN, PSI, CH KVI, Groningen, NL	HIF, UCL, B
MSI SWIR2	ESTEC, Noordwijk, NL ESTEC, Noordwijk, NL	PROSCAN, PSI, CH KVI, Groningen, NL	HIF, UCL, B

Ionizing Radiation Results.

In none of the experiments, latch-up effects were seen during ^{60}Co radiation.
The following parameters were followed during the radiation testing:

- Changes in overall power consumption
- Changes in dark current
- Changes in noise

The power dissipation remains constant under all irradiation conditions. For the MSI as well as the Proba-V devices, the reset reference point hardly moves.

The dark current of the MSI-SWIR 1 devices tends to increase with some 75% after 10 krad(Si) dose (see Figure 5):

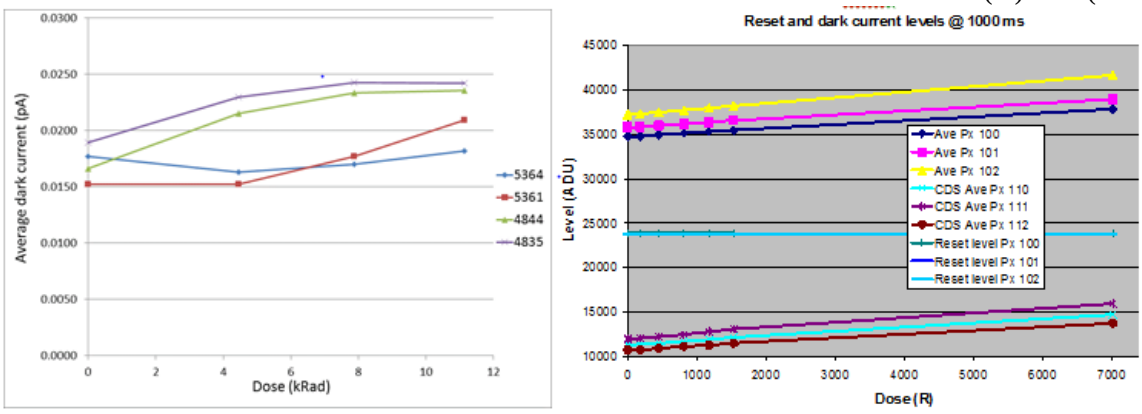

Figure 5: Left: Change in dark current as a function of ionizing radiation dose. Device 5364 is the reference device. Right: comparison with dark current results measured in 2004.

The noise of all SWIR1 devices (MSI as well as Proba-V) remains unchanged after a 10 krad(Si) dose (see Table 3).

Table 3: Parameter shifts after ^{60}Co radiation.

	RED				NIR				SWIR2			
	REF	**5856**	**5861**	**5863**	**REF**	**5877**	**5885**	**5891**	**REF**	**4847**	**4858**	**4860**
Noise [e-]	99.5%	99.5%	99.6%	99.2%	99.6%	100.2%	100.0%	99.3%	103.5%	97.3%	103.9%	103.7%
Idark [pA]	103.5%	145.5%	160.3%	160.6%	62.6%	157.1%	182.8%	147.2%	109.1%	104.8%	134.4%	93.4%
Linearity	97.4%	93.8%	96.4%	90.1%	90.5%	95.4%	95.9%	96.1%	67.0%	97.0%	143.5%	125.8%

The noise and the linearity of the devices remains essentially unchanged, whereas the dark current has a tendency to increase with app. [50-60%].

Proton Testing.

The high energy proton test with energies > 100 MeV are mainly intended to test the ROIC for SEE immunity. In both cases (Proba-V and MSI) high energy protons could not provoke latch-up.

In the SWIR1 case, the high energy and certainly the low energy protons are causing a change in the dark current of the devices, such as illustrated in Figure 6 for the Proba-V and the MSI case.

For the MSI RED and NIR devices the increase in dark current is equivalent. For the MSI SWIR2 devices the effect of proton dose is less pronounced, as indicated in Figure 7.

In none of the cases the noise, responsivity, PRNU nor the power dissipation is meaningfully changed by the proton dose.

Mainly in the SWIR2 FPAs some pixels are showing a RTN (Random Telegraph Noise) behaviour. This behaviour is not changed under the influence of proton fluence (see Figure 8).

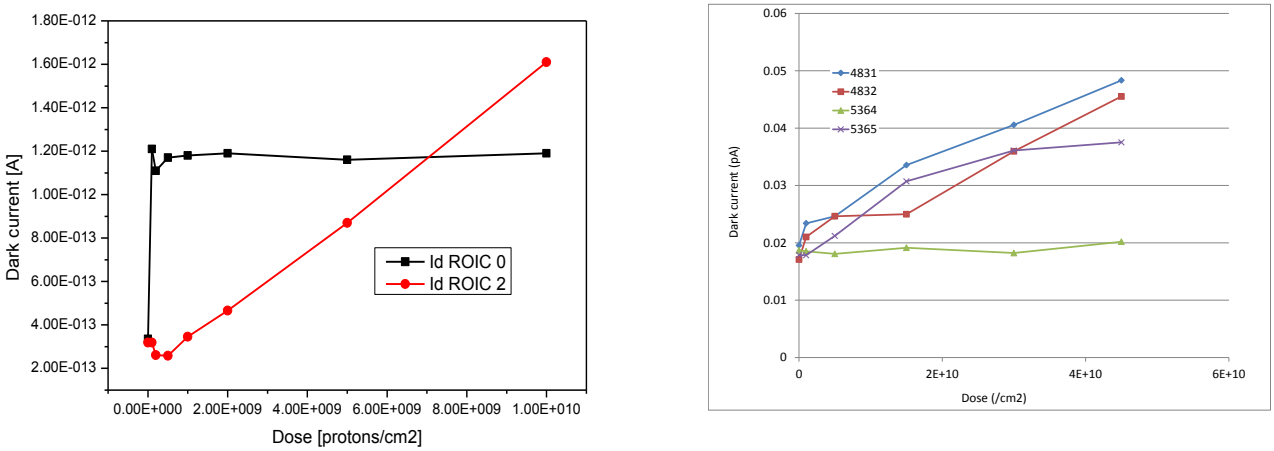

Figure 6: Dark current behaviour under the influence of high energy proton fluence. Left: Proba-V FPA. Right: MSI SWIR1 FPA. 5364 is the non-exposed reference device.

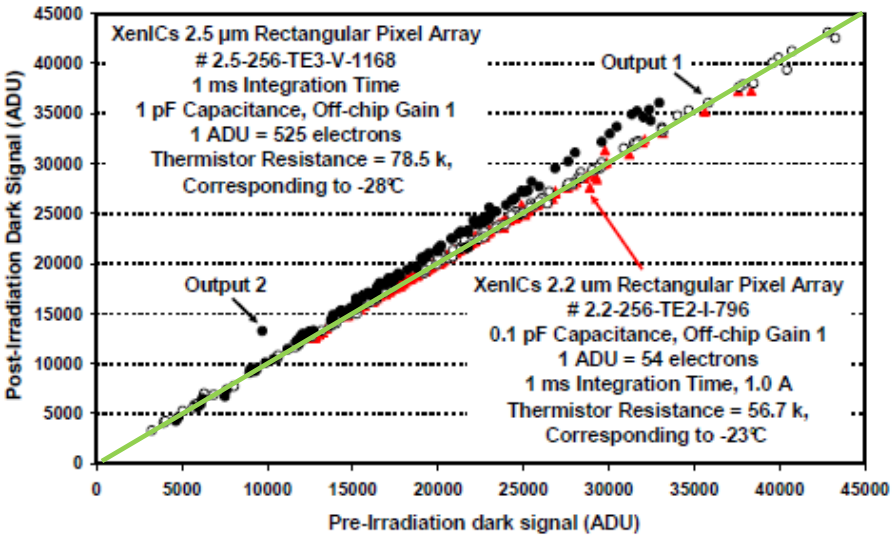

Figure 7: Dark signal for each photodiode after 1.5*10^{10} p/cm2 proton irradiation with an energy of 60 MeV versus the dark signal before irradiation for both 2.5 µm (open symbols) and 2.2 µm arrays (filled triangles), obtained with 1 pF and 0.1 pF integration capacitance, respectively. Integration time = 1 ms. (Picture courtesy of SSTL)

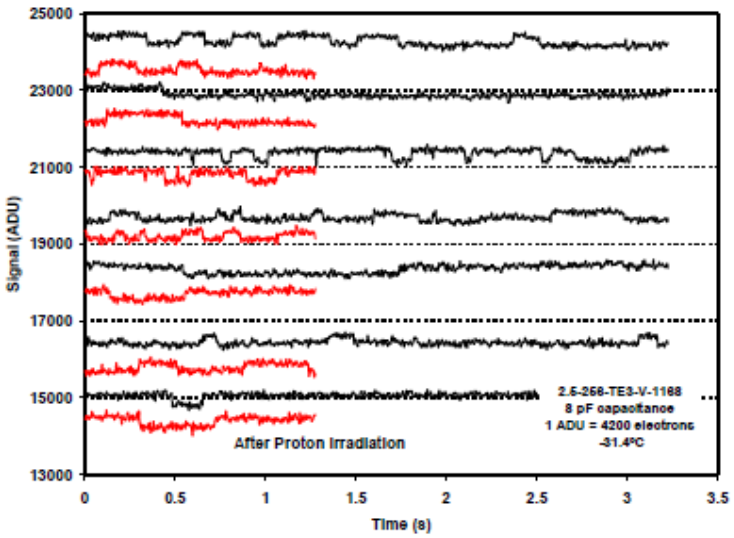

Figure 8: Dark signal versus time for 2-level RTS pixels both before (long traces) and after irradiation (short traces), for the 2.5µm array. The plots have been offset vertically for clarity. (Picture courtesy of SSTL)

Heavy Ion Testing

Both the ROICs for Proba-V and for the MSI mission are designed as commercial products. This makes both ROICs potentially susceptible to SEE. On the other hand the on-chip logic is rather simple in order to allow easy sequence optimization. This implies that both circuits are not fully SEE safe, but show sufficient heavy ion resistance to allow space operation, when sufficiently protected by external means, such as latch-up detection circuits and automatic reboot circuitry.

The observed SEE's can be categorized in 3 categories:

- Single Event Functional Interrupts or SEFI's, where a (part of a) line is destroyed by the particle transition, but the device returns to regular operation at the next readout. An example of a sequence of SEFI's is given in the top part of Figure 9.

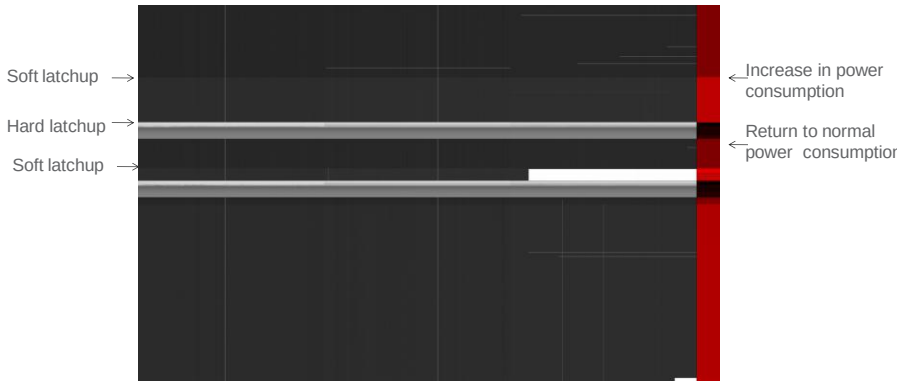

Figure 9: Example of SEFI's, soft and hard latch-ups detected by the EGSE during irradiation. The red vertical line is a measure for the FPA current.

- Soft latch-ups, where the FPA come into a state, which is obviously wrong, but keeps operating: e.g. the average intensity level becomes too bright. In most cases this situation is characterized by a slight power increase, which can be detected by the external housekeeping electronics. Some cases are recorded where an increase in current is measured without direct implication for the image quality.
- Hard latch-ups where the FPA stops functioning and the power consumption increases till the compliance level.

DISCUSSION

The ^{60}Co has mainly an influence on the dark current of the detectors. As no change in output level for unconnected pixels is seen, it can be safely concluded that the dark current increase is coming from the detectors (most probably from an increase in Generation-recombination (G-R) current).
The dark current increase is less visible on the SWIR2 PDAs: leading to the conclusion that the material defects, mainly dislocations affect, are not affected.

The proton effects have to be divided in 2 classes:

- The low energy protons, causing displacements effects mainly in the PDA's
- The high energy protons, affecting the proper functioning of the ROIC by causing SEE.

An increase in dark current is certainly observed for the low energy protons. We see a difference in behaviour between the Proba-V and the MSI FPA (an increase with a factor 10 after 10^{10} p^+/cm^2 for Proba-V versus a factor of 2 for MSI). It is believed that the detector bias is important here:

- The Proba-V ROIC is designed to operate with a detector bias of [0.1 – 0.4 V],
- The MSI ROIC is designed for interfacing SWIR2 detectors with a low R_oA, operating with an effective detector bias in the [-20 - +20 µV] range.

These differences can explain the behaviour of the FPA:

- Due to the higher bias for the Proba-V detectors, the starting dark current is already one order of magnitude higher.
- The back-bias will also increase the space charge region of the photodiode and hence give rise to a higher semiconductor volume available for the G-R current,
- A change in G-R rate under the influence of proton fluence, will hence affect more the photodiodes with the largest space charge region.

The high energy protons are not producing enough charge in the Silicon substrate of the ROIC to cause any SEE problems. This is valid for all ROICs and detector materials.

The heavy ions are almost uniquely affecting the performance of the ROIC. Although the FPAs are equipped with ROICs from a different technology, the cross-section is almost equal:
$\sigma \approx [10^{-5} - 10^{-4}\ cm^2]$ for LET $\approx$ [30 – 40 MeV/cm^2/mg(Si)]. The main reason is that the architecture of both ROICs is very comparable: both have a minimal on-board sequencer. The most important digital circuitry is the delay line for the selection of the pixels, designed as a static shift register, which does not contain high impedance, dynamic storage nodes. This design approach reduces strongly the latch-up susceptibility of the ROIC. Even when one storage node is changing state under the influence of an incident ion, this will normally not cause a hard latch-up; by the introduction of

an additional selection bit, the power consumption will slightly rise and the (dark) output level will be slightly affected without causing saturation.

Most important is that radiation does not introduce additional pixels, affected by RTN [16-18].

CONCLUSIONS

The degradation of the FPA's is measured for ionizing and non-ionizing radiation. The influence of a ^{60}Co life time dose on dark current is noticeable, for low energy protons a dark current increase is also observed. The dark current increase is strongly dependent on the detector backbias and points to an increase in GR rate in the space charge region of the photodiodes

High energy protons have a smaller influence on the dark. High energy protons are not capable of creating SEE in either of both presented FPA types.

Heavy ions are causing both SEFI, as well as soft and hard latch-ups. The first two types of SEE are rather harmless for the circuit since they only cause a small current increase in the ROIC; the FPA can be protected by an external current limiting circuit against hard latch-ups.

None of the detector materials, nor any of the applied ROIC's give rise to an increase in RTN pixels.

ACKNOWLEDGEMENTS

The authors want to thank their colleagues at ESA-ESTEC, the involved Proba-V team members at Qinetiq Space, OIP and VITO as well as the MSI team members at TNO, Dutch Space, SSTL and Astrium for the many helpful discussions. They want to explicitely mention the late Gordon Hopkinson for his detailed pre-analysis of the MSI FPA's under ESA contract 20232/06/NL/FF. They also thank their colleagues at Xenics for their efforts in InGaAs processing and characterization, FPA assembly and for the test and qualification efforts.

REFERENCES

[1] Maisongrande P. et Al. (2010) PROBA-V , *A Satellite for the Continuity of the SPOT/VEGETATION Mission*, Geophysical Research Abstracts, Vol 12, EGU2010-14202-1

[2] EarthCARE Mis. Adv. Group, *EARTHCARE: Mission requirements document*, EC-RS-ESA-SY-012, Nov 2006

[3] S. Katagiri et Al., *Earthcare science mission requirements*, International Archives of the Photogrammetry, Remote Sensing and Spatial Information Science, Volume XXXVIII, Part 8, Kyoto Japan 2010

[4] A. Rogalski, *Infrared Handbook – Second Edition*, CRC Press, 2011

[5] T. R. Gentile, *Internal QE modeling of silicon photodiodes*, Applied Optics, Vol 49, No 10, pp 1859, 2010

[6] Vermeiren J (2009) A fast 1024 pixel, 12.5 um Pitch InGaAs array for FBG sensing applications, SPIE Vol 7474

[7] J. John et Al., *Extended InGaAs on GaAs Detectors for SWIR Linear Sensors*, SPIE Infrared Technology and Applications XXVII, Vol 4369, 2001

[8] O. Lapshinov et al., *Design, development and first assessment of the SWIR instrument for remote sensing on board of egyptsat-1*, Proc. 4S Conference, Rhodes, 2008

[9] J. Vermeiren, *III-V Microsystems for IR imaging and spectroscopic applications*, SPIE Conf 4947, Bruges 2002.

[10] William D. Rogatto, *The Infrared handbook, Vol 3*, SPIE, 1999

[11] De Vos L. et Al., *The Vegetation Instrument for the PROBA V Mission*, Proc. 7th IAA Symposium on Small Satellites for Earth Observation, Berlin, 2009

[12] A. Hoffman, *Capacitor Transimpedance amplifier (CTIA) with shared load*, US Patent 6252462, 2001

[13] M. Ettenberg et Al., *InGaAs imaging with smaller cameras, higher resolution arrays and greater material sensitivity*, proc SPIE 4721-03, 2002

[14] Pimbley, J.M. & Michon, G.J., *The output power spectrum produced by correlated double sampling, Circuits and Systems*, IEEE Transactions on, Vol. 38, 1991

[15] Paul W. Marshall & Cheryl J. Marshall, *Radiation Damage Mechanisms in CCD Imagers*, STScI Workshop on HST CCD Detector CTE, 31 Jan – 01 Feb 2000

[16] O. Amore et Al., *InGaAs SWIR imaging detectors hardening against proton irradiation*, B. Andresen, G. F. Fulop, and M. Strojnik, SPIE vol. 4820, no. 1. pp. 436-445, 2003

[17] J.S. Kolhatkar et Al., *Separation of Random Telegraph Signals from 1/f Noise in MOSFETs under Constant and Switched Bias Conditions*, Proc ESSCIRC, 2003

[18] A.P. van der Wel et Al., Relating random telegraph signal noise in metal-oxide-semiconductor transistors to interface trap energy distribution, Appl. Phys. Let. 87, No18, pp3507, 2005